32nd URSI GASS, Montreal, 19-26 August 2017

Conjugate ground-satellite ELF/VLF emissions observed with strong magnetospheric compression

Claudia Martinez-Calderon*(1)(2), Kazuo Shiokawa (2), Kunihiro Keika (3), Satoshi Kurita (2), Mitsunori Ozaki (4), Ian Schofield (5), Martin Connors (5), Craig Kletzing (6), Ondrej Santolik (7,8) and William S. Kurth (6)
(1) Department of Geophysics, Graduate School of Science, Tohoku University
(2) Institute for Space-Earth Environmental Research, Nagoya University, Japan
(3) Department of Earth and Planetary Science, Graduate School of Science, University of Tokyo, Japan
(4) Faculty of Electrical and Computer Engineering, Institute of Science and Engineering, Kanazawa University, Japan
(5) Athabasca University Observatories, Athabasca, Alberta, Canada.
(6) Department of Physics and Astronomy, University of Iowa, Iowa, USA
(7) Faculty of Mathematics and Physics, Charles University, Prague, Czech Republic
(8) Institute of Atmospheric Physics, Czech Academy of Sciences, Prague, Czech Republic

Abstract

We report the first simultaneous ground and satellite conjugate observations of ELF/VLF waves associated with magnetospheric compression. On 23 December 2014, a receiver at subauroral latitudes at Athabasca (ATH), Canada (54.7N, 246.7E, L=4.3) observed an ELF/VLF wave burst centered at ~2.5 kHz. This emission showed discrete elements and lasted ~3 minutes starting at 11:17 UT (~2.4 MLT). RBSP-B, located nearly conjugate to ATH in the post-midnight sector (~3 3 MLT) observed a similar emission. This wave burst was observed a few minutes after an intense sudden impulse (SYM-H amplitude ~53 nT) caused by the enhancement of solar wind speed (~330 to ~420 km/s) and dynamic pressure (~2 to 6 nPa) during northward IMF. At 11:16 UT, RBSP-B also observed a separate hiss emission below 1.5 kHz that was not observed at ATH. We investigate the possible generation mechanisms of these waves and suggest that they differ for the hiss and discrete emissions and that their propagation to the ground is also different.

1. Introduction

A sudden impulse (SI) is characterized by a clear onset that is detected everywhere in the magnetosphere [1]. It is defined as the sharp increase of either of the components of the horizontal magnetic field at low latitudes stations of at least 10 nT in amplitude in 3 minutes or less [2]. Whistler mode waves are naturally occurring right handed plasma waves in the magnetosphere propagating at frequencies below the local gyrofrequency of electrons. They can propagate in this mode at extremely low (ELF) to very low (VLF) frequency bands (30 Hz to 30 kHz). They may be classified using their spectral features, for example discrete chorus, incoherent emissions like hiss or periodic and quasi-periodic emissions among others [3]. As they propagate from their generation region near the magnetosphere's geomagnetic equator they can interact with relativistic electrons in the radiation belts causing their acceleration or loss [4,5]. Some studies have correlated the enhancement of chorus amplitude with global compression of the magnetosphere due to betatron acceleration of high-energy electrons resulting in enhancement of temperature anisotropy [6]. There are also cases that were not accompanied by any change in the anisotropic electron distribution [7]. This study shows the generation of two types of wave, an initial hiss emission followed a minute later by a burst showing discrete features that took place in the post-midnight sector. We use polarization and wave analysis on the ground and in space, combined with electron flux and density data to discuss the characteristics of the generation ELF/VLF waves during an SI event. The full results reported in this extended abstract are summarized into a manuscript and submitted to the Journal of Geophysical Research as Martinez-Calderon et al. (2017) [23].

2. Data and Observations

Ground-based observations were made at the Athabasca University Geospace Observatory (54.60N, 246,36E, MLAT=61.14N, L=4.3) in Canada using a high sampling rate (100 kHz) delta-type loop antenna [8,9]. We use magnetic field data from the AUTUMN magnetometer network at their Athabasca site (54.71N 246.68E) [10]. Satellite-based observations were made by the Van Allen Probe B, (RBSP-B) using the The Electric Fields and Waves Instruments providing wave electric and magnetic field data [11] and The Energetic Particle Composition and Thermal Plasma Suite providing electron flux data and pitch angle distributions [12].

On 23 December 2014, at 11:15 UT, we observed a clear and sudden increase of solar wind speed from ~330 to 440 km/s, dynamic pressure from ~2 to 6 nPa and a ~53 nT amplitude increase of SYM-H with northwards IMF-Bz. This is characteristic of a SI+ event. A few minutes afterwards, ATH observed a wave burst from ~11:17 UT to ~11:20 UT centered at ~2.5 kHz and showing discrete features (Figure 1a). This discrete emission was highly coherent (> 0.6) and highly right-hand (RH) polarized, the latter suggesting the wave was coming directly from the ionosphere. The polarization angle values indicate that the

ionospheric exit point was located westwards of ATH. Figure 1b shows the variations of the three components of the magnetic field. The sudden increase of the H-component, characteristic of an SI, is also observed at ATH. At this time, RBSP-B was in the southern hemisphere moving inwards and ~ 3 to 4º below the geomagnetic equator, outside of the plasmapause. The footprint of the satellite was ~750 km northwest of the ground-station. Both the RBSP-B and ATH were located on the post-midnight side (~02-03 MLT). The spectrogram of RBSP-B on Figure 1c shows two separate emissions: (1) Hiss starting at 11:16 UT, centered around 0.8 kHz with an approximate bandwidth of 1.5 kHz. (2) Discrete emission starting at 11:17 UT, centered at ~2.2 kHz. The gray dashed vertical lines on Figure 2 indicate the starting time of each emission. Although we do not observe the exact same discrete elements at ATH, the wave in both locations has the same frequency, same timing and overall shape. The fact that we cannot match internal discrete elements between the ground and space can be explained by dispersion, varying propagation properties or even noise pollution. We can assume that for the discrete emission, ATH and RBSP-B are observing the same emission at the same time, making this a conjugate event.

Using the same analysis detailed in [9] we calculated polarization parameters. The discrete emission had a frequency dependence of the wave vector angle, with lower frequencies having oblique wave angles (>60º) while higher frequencies had smaller angles with respect to the field line. We calculated the resonance cone for the minimum, maximum and central frequencies and found that for the discrete emission they vary between 40º and 75º. Thus the wave vector angle are within 15º to 2º from the resonance cone, in agreement with [13] who found that lower band chorus in its source region can in some cases propagate at highly oblique angles, close to the resonance cone. Figure 1d shows the variations for each magnetic field component measured by RBSP. The starting time of the hiss corresponds to the start of the magnetic field amplitude increase. Figure 1e shows the variations with time of the elevation angle theta. At the time of the SI the angle starts decreasing from 54º to 49º, suggesting RBSP-B was observing a tailward stretching of the magnetic field.

We use the methods described in [14] and [15] to calculate the minimum resonance energy: ~2-40 keV for the hiss and few hundred eV to 4 keV for the discrete emission. Figure 1f shows the temperature for electrons with energies above 200 eV. The perpendicular (T_{perp}) and parallel temperatures (T_{par}) are shown with blue and red lines respectively. Figure 1g shows the ratio of T_{perp}/ T_{par} for electrons with energies greater than 30 eV. The ratio remains fairly stable with values close to 1.4, with no sudden increase of T_{perp} before the start of any of the emissions. Figure 1h shows the electron flux from the HOPE separated by energy channels (16.8 eV to 2.9 keV), while Figure 1i shows it for MagEIS (75 and 743 keV). For energies below 166.9 eV there is a sudden increase of flux at the start time of the hiss, continuing beyond the end of the discrete emission. For 296.2 eV and 2.9 eV we see a generally stable flux (except for the 1.6 keV channel). At energies above 75 keV we observe flux enhancements at the same time as the hiss emission (except for the 2.6 MeV channel).

Solid lines indicate pitch angle distribution before the start of the emission, while dotted and dashed lines are timed after the hiss and discrete emission, respectively. Figure 2 shows the electron flux as a function of pitch angle and energy from both the HOPE and MagEIS instruments. The solid lines correspond to the pitch angle distribution before the start of both emissions, while the dotted and dashed lines correspond to the times after the hiss and discrete emission, respectively. In all cases, except for the 1.47 keV, we see a global increase of the electron flux for all pitch angles. In particular for the 0.83 keV channel, which is the closest to the minimum resonance energy for the discrete emission, we note a larger increase of the flux t 90^{o} pitch angle.

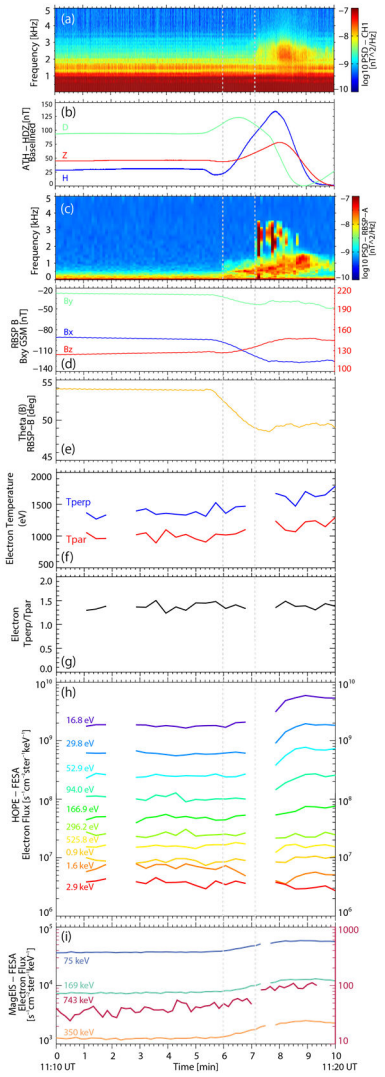

Figure 1. (a) PSD and (b) magnetic field variations at ATH (c) PSD and (d) magnetic field variations at RBSP-B (e) Variations of elevation angle theta (f) Parallel and perpendicular electron temperatures given by HOPE and (g) their ratio (h) Electron flux for energy channels between 16.8 eV and 2.9 keV and (i) between 75 and 743 keV.

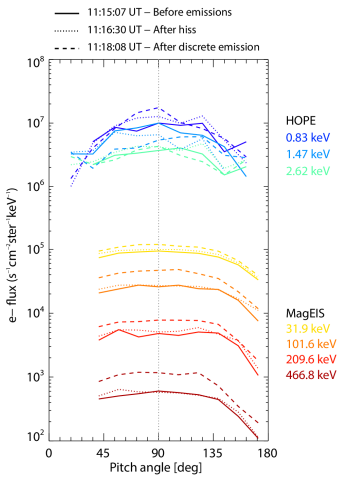

Figure 2. Electron flux as a function of pitch angle for 0.83 to 2.62 keV (HOPE) and 31.9 to 466.8 keV (MagEIS).

3. Discussion

3.1 Generation Mechanism

Injection of anisotropic electrons and protons with energies between 10 and 100 keV by substorms, could be a mechanism for generation of waves such as those we observed [16,17]. However, THEMIS A, E and D located on the dusk side, do not show proton injection. The ground station of Magadan (MGD, 51.9 MLAT, 60N, 150E) located at 20 MLT at the time of the event did not record Electromagnetic Ion Cyclotron (EMIC) wave activity, commonly associated with substorms. ATH does not detect any EMIC activity either, suggesting we can rule out a post-midnight particle injection.

As the magnetosphere is compressed by the SI, the conservation of the first adiabatic invariant causes betatron acceleration of high-energy electrons and an initial rise in the electron fluxes at constant energy (Figure 1h-i). This is usually accompanied by an increase of the T_{perp} anisotropy. However, as shown in Figures 1f-g, we do not see any significant increase of the temperature anisotropy. Usually, $T_{perp}/T_{par}>1$ is necessary as free energy to generate whistler mode waves, but is not the only factor regulating wave growth. Linear wave growth rate can be altered by the ratio of electron flux over phase space density [18]. As the adiabatic acceleration moves the energy spectrum towards higher energies, the flux over phase space density for a given energy increases. Even though strong anisotropy is needed for wave generation, its increase itself is not essential. On the contrary, [7] found that even though chorus enhancement was observed associated with an IP shock and increase of the background magnetic field, the electron anisotropy and pitch angle distribution remained globally unchanged. Instead of the chorus being excited by the increase of available energy, it was likely enhanced by the decrease of the threshold required to excite chorus. This hypothesis might explain the delay between the generations of the two types of waves. As the compression moves through the magnetosphere, RBSP-B observes tailward stretching, suggesting that the source region of the waves might be subject to radial motion. As such RBSP-B might not be able to see the sudden increase of T_{perp} but was still able to see the waves after they reflected in the magnetosphere. Even though T_{perp} increased, another mechanism may have made T_{par} increase at the same time. GOES-13 and GOES-15, on the dawn and pre-midnight sector respectively, detected a flux increase for electrons between 40 and 150 keV. The minimum resonance energy at which an electron can interact with the waves is within this range. The 40 keV energy channel is close to the source energy of the waves observed by RBSP-B, suggesting these electrons can be a possible energy source for the emissions.

Chorus generation and their spectral characteristics are affected by the spatial inhomogeneity of the background magnetic field [19]. Smaller inhomogeneities along the magnetic field lines led to broadband hiss-like emission. As the magnetosphere is compressed by the SI, the magnetic curvature at the geomagnetic equator, source of the emissions, is reduced. This corresponds to smaller inhomogeneities along the field line, making conditions more favorable to the generation of hiss-like emissions. RBSP-B detected the hiss emission just a few minutes after the SI and one minute earlier than the discrete emission. As time progresses, the elevation angle decreases steadily suggesting that the satellite is observing tailward stretching, increasing the magnetic curvature at the equator and making the conditions more favorable for chorus-like emissions. Previous studies have determined that there is a connection between chorus and hiss, showing that plasmaspheric hiss can come from transformed chorus waves [20]. The generation of the hiss might be linked to dayside chorus which propagated and leaked into the plasmasphere to ATH at the post-midnight sector, explaining the time delay between the observations of the two emissions.

3.2 Propagation

ATH observed a discrete emission a few minutes after the SI, incoming westwards and strongly RH polarized suggesting the waves were coming directly from the ionosphere. At the same time, RBSP-B shows a similar discrete emission, RH polarized with southward Poynting flux and oblique wave angles. For chorus waves to penetrate the ionosphere unducted, they require large wave vector angles at the equatorial source [21,22]. We suggest that the discrete emission was most likely generated at the equator by a symmetrical source. Some of the waves propagated northward unducted to ATH, while others continued southward to RBSP-B. A minute earlier, RBSP-B observed a hiss emission at lower frequencies that was not observed on the ground. The hiss was RH polarized, Poynting flux northwards and small wave angles. We suggest that this emission was probably generated at a source located inward or outward from the L-shell of RBSP-B, reflected near the ionosphere and was detected by the satellite afterwards. After it propagated to other L-shells as it continued to be reflected in the magnetosphere

until it either dissipated or exited to the ionosphere at a different point than ATH.

4. Acknowledgements

ELF/VLF data is available at http://stdb2.stelab.nagoya-u.ac.jp/vlf/index2.html. We thank Y. Katoh, H. Hamaguchi, Y. Yamamoto, T. Adachi, M. Sera and Y. Ikegami of ISEE, as well as K. Reiter from Athabasca University, for their continued technical support. The Athabasca University Geospace Observatory facilities are supported by the Canada Foundation for Innovation. Fluxgate magnetometer data can be found at http://autumn.athabascau.ca/ and http://supermag.jhuapl.edu/. RBSP satellite data can be found at the EMFISIS (http://emfisis.physics.uiowa.edu/Flight/), MagEIS and HOPE database (https://rbsp-ect.lanl.gov/data\pub/). Solar wind parameters and GOES data were obtained from SPDF/GSFC OMNIWeb (http://omniweb.gsfc.nasa.gov/form/omni\min.html). This work was supported by the IUGONET of the Japanese Ministry of Education, Culture, Sports, Science and Technology, the Grant-in-Aid for Scientific Research from the Japan Society for the Promotion of Science and by the Leadership Development Program for Space Exploration and Research at Nagoya University. The work done at the Charles University and at the Institute of Atmospheric Physics in Prague has been supported from the LH14010 and GACR 14-31899S grants and by the Praemium Academiae award. The research at University of Iowa was supported by JHU/APL contract 921647 under NASA prime contract NAS5-01072.

5. References

[1] T. Araki, "A physical model of the Geomagnetic sudden commencement," in Solar Wind Sources of Magnetospheric Ultra-Low-Frequency Waves. Wiley-Blackwell, 2013, pp. 183–200.

[2] J. A. Joselyn and B. T. Tsurutani, "Geomagnetic sudden impulses and storm sudden commencements: A note on terminology," Eos, Transactions American Geophysical Union, vol. 71, no. 47, p. 1808, 1990.

[3] R. A. Helliwell, Whistlers and related ionospheric phenomena. Mineola, NY: Dover Publications, 2006.

[4] R. M. Thorne, "Radiation belt dynamics: The importance of wave-particle interactions," Geophysical Research Letters, vol. 37, no. 22, p. Nov. 2010.

[5] M. Hayosh, D. L. Pasmanik, A. G. Demekhov, O. Santolik, M. Parrot, and E. E. Titova, "Simultaneous observations of quasi-periodic ELF/VLF wave emissions and electron precipitation by DEMETER satellite: A case study," Journal of Geophysical Research: Space Physics, vol. 118, no. 7, pp. 4523–4533, Jul. 2013.

[6] K. Shiokawa et al., "Ground-based ELF/VLF chorus observations at subauroral latitudes VLF-CHAIN campaign," Journal of Geophysical Research: Space Physics, vol. 119, no. 9, pp. 7363–7379, Sep. 2014.

[7] C. Zhou et al., "Excitation of dayside chorus waves due to magnetic field line compression in response to interplanetary shocks," Journal of Geophysical Research: Space Physics, vol. 120, no. 10, pp. 8327–8338, Oct. 2015.

[8] M. Ozaki et al., "Localization of VLF ionospheric exit point by comparison of multipoint ground-based observation with full-wave analysis," Polar Science, vol. 2, no. 4, pp. 237–249, Dec. 2008.

[9] C. Martinez-Calderon, K. Shiokawa, Y. Miyoshi, M. Ozaki, I. Schofield, and M. Connors, "Polarization analysis of VLF/ELF waves observed at subauroral latitudes during the VLF-CHAIN campaign," Earth, Planets and Space, vol. 67, no. 1, p. 21, 2015.

[10] S. B. Mende et al., "The THEMIS array of ground-based Observatories for the study of Auroral Substorms," Space Science Reviews, vol. 141, no. 1-4, pp. 357–387, Jun. 2008.

[11] C. A. Kletzing et al., "The electric and magnetic field instrument suite and integrated science (EMFISIS) on RBSP," Space Science Reviews, vol. 179, no. 1-4, pp. 127–181, Jun. 2013.

[12] H. E. Spence et al., "Science goals and overview of the radiation belt storm probes (RBSP) energetic particle, composition, and thermal plasma (ECT) suite on NASA's Van Allen Probes mission," Space Science Reviews, vol. 179, no. 1-4, pp. 311–336, Oct. 2013.

[13] O. Santolík, M. Parrot, U. S. Inan, D. Burešová, D. A. Gurnett, and J. Chum, "Propagation of unducted whistlers from their source lightning: A case study," Journal of Geophysical Research: Space Physics, vol. 114, no. A3, p., Mar. 2009.

[14] W. Li et al., "THEMIS analysis of observed equatorial electron distributions responsible for the chorus excitation," Journal of Geophysical Research: Space Physics, vol. 115, no. A6, p, Jun. 2010.

[15] W. S. Kurth et al., "Electron densities inferred from plasma wave spectra obtained by the Waves instrument on Van Allen Probes," Journal of Geophysical Research: Space Physics, vol. 120, no. 2, pp. 904–914, Feb. 2015.

[16] B. T. Tsurutani and X. Zhou, "Interplanetary shock triggering of substorms: WIND and polar," Advances in Space Research, vol. 31, no. 4, pp. 1063–1067, Jan. 2003.

[17] K. Keika et al., "Substorm expansion triggered by a sudden impulse front propagating from the dayside magnetopause," Journal of Geophysical Research: Space Physics, vol. 114, no. A1, Jan. 2009.

[18] W. Li, R. M. Thorne, J. Bortnik, Y. Nishimura, and V. Angelopoulos, "Modulation of whistler mode chorus waves: 1. Role of compressional Pc4-5 pulsations," Journal of Geophysical Research: Space Physics, vol. 116, no. A6, Jun. 2011.

[19] Y. Katoh and Y. Omura, "Effect of the background magnetic field inhomogeneity on generation processes of whistler-mode chorus and broadband hiss-like emissions," Journal of Geophysical Research: Space Physics, vol. 118, no. 7, pp. 4189–4198, Jul. 2013.

[20] J. Bortnik, R. M. Thorne, and N. P. Meredith, "The unexpected origin of plasmaspheric hiss from discrete chorus emissions," Nature, vol. 452, no. 7183, pp. 62–66, Mar. 2008.

[21] J. Chum and O. Santolík, "Propagation of whistler-mode chorus to low altitudes: Divergent ray trajectories and ground accessibility," Annales Geophysicae, vol. 23, no. 12, pp. 3727–3738, Dec. 2005.

[22] C. Martinez-Calderon et al., "ELF/VLF wave propagation at subauroral latitudes: Conjugate observation between the ground and Van Allen Probes A," Journal of Geophysical Research: Space Physics, vol. 121, no. 6, pp. 5384–5393, Jun. 2016

[23] C. Martinez-Calderon et al., "Conjugate ground-satellite ELF/VLF emissions generated by strong magnetospheric compression," submitted to J. Geophys. Res., 2017.